Progress in Nuclear Energy 53 (2011) 1034–1038

Contents lists available at ScienceDirect

Progress in Nuclear Energy

journal homepage: www.elsevier.com/locate/pnucene

Scale removal oxidation behavior of metal in supercritical water modeled by cellular automaton

Kuan-Che Lan [a], Yitung Chen [b], Tsung-Kuang Yeh [a,c], Tzu-Chen Hung [d], Ming-Lou Liu [e], Ge-Ping Yu [a,c,*]

[a] Department of Engineering and System Science, National Tsing Hua University, No.101, Section 2, Kuang Fu Road, Hsinchu 300, Taiwan, R.O.C
[b] Department of Mechanical Engineering, University of Nevada, Las Vegas, 4505 Maryland Parkway, Box 454027, Las Vegas, NV 89154-4027, United States
[c] Institute of Nuclear Engineering and Science, National Tsing Hua University, No.101, Section 2, Kuang Fu Road, Hsinchu 300, Taiwan, R.O.C
[d] Department of Mechanical Engineering, National Taipei University of Technology, No. 1, Sec. 3, Chung-Hsiao E. Rd., Taipei 106, Taiwan, R.O.C
[e] Department of Civil and Ecological Engineering, I Shou University, No.1, Sec. 1, Syue-Cheng Rd., Dashu District, Kaohsiung City 84001, Taiwan, R.O.C

ARTICLE INFO

Article history:
Received 21 October 2010
Received in revised form
30 January 2011
Accepted 28 April 2011

Keywords:
Scale removal
Mesoscopic
Cellular automaton
Oxidation
Supercritical water
Inconel 625

ABSTRACT

Corrosion and oxidation of structure material in supercritical water are specific and an important issue in the nuclear industry. A scale removal cellular automaton model was proposed to investigate the development of a continuous oxide layer of Inconel 625 in supercritical water at 24.8 MPa and 600 °C. This study presented influence of the reaction behavior of oxidation, scale removal effect, and transport ratio of oxygen and metal ions on the corrosion and oxidation process with different conditions. The formation of the spinel is simulated at mesoscopic level. The developed model is also mapped with the laboratory experimental data from a supercritical water loop.

1. Introduction

Supercritical water reactor (SCWR) is one of the advanced reactors designed for Generation IV nuclear reactors. Under high temperature supercritical water, nickel based alloy are proposed as a candidate structural materials for SCWR to sustain the severe oxidation and corrosion. Among the nickel based alloy, Inconel 625 superalloy has been applied to the aerospace, chemical industry and pilot-scale nuclear system (Otsuka and Fujikawa, 1991). However, such high working temperature (upto 600 °C) of the supercritical water would bring serious damage to structure material such as oxidation and corrosion. The oxidation and corrosion of the structure material under high temperature is complex and have to be investigated in detail before the superalloy applied on SCWR. Using the viewpoint of an atom and molecular to simulate a macroscopic problem like oxidation and the growth of nickel based alloy in supercritical water is time consuming and a tough challenge. The mechanism of oxidation and the growth of oxide layer of the nickel based structure materials in supercritical water has been discussed (Wasa et al., 2007; Tan et al., 2008a; Sun et al., 2008). However, these experimental studies demonstrate the fact that these kinds of researches are hard to be achieved at a microscopic level by means of approaches of computation fluid dynamics in the field of fluid mechanics. Thus, developing another economic and physically reasonable approach of computer simulation of the growth of the oxide layer in high temperature supercritical water at a mesoscopic scale is worth performing. Our mesoscopic oxidation model has been successfully achieved to study the corrosion and oxidation of stainless steel in the eutectic lead bismuth flow (Tan et al., 2008c, 2008b; Tan and Chen, 2009b, 2009a). Following the concept of numerical simulation at mesoscopic view, the objective of this study is to develop an approach to investigate the oxidation behavior of nickel based alloy in supercritical water. The results will be beneficial and important for future study of the metal oxidation.

A theoretical model which can elaborate the interface growth process was proposed by Eden (Eden, 1961). Then Eden's model was extended by Saunier, who built a simple cellular automaton (CA) model where the diffusion of iron was the only specie of structure materials to be taken into consideration (Saunier et al., 2004). The goal of Saunier's simple CA model was to study the effect of kinetic parameters involved in the corrosion mechanisms on the corroded surface roughness (Saunier et al., 2004). There was disregard of

* Corresponding author. Department of Engineering and System Science, National Tsing Hua University, No.101, Section 2, Kuang Fu Road, Hsinchu 300, Taiwan, R.O.C. Tel.: +886 3 5715131; fax: +886 3 5720724.
E-mail address: gpyu@ess.nthu.edu.tw (G.-P. Yu).

0149-1970/$ – see front matter © 2011 Elsevier Ltd. All rights reserved.
doi:10.1016/j.pnucene.2011.04.020

presence of the oxygen in flow and the inner reaction between the metal and oxide interface. Recently, Chen and Tan proposed an improved mesoscopic oxidation (IMO) CA model where the effect of the oxygen was involved (Tan et al., 2008c). In Chen and Tan's improved CA model, the transport of oxygen was considered and was assumed to transport along the grain boundaries. They found that the oxygen does significant influence on the growth of the oxide layer in which the reactions take place on the oxide/liquid interface, on the steel/oxide interface, and even inside the oxide films as well.

An advanced IMO CA model which considered more about the hydraulic effect has been developed by Chen and Tan (Tan and Chen, 2009) where the basic study of corrosion and oxidation of structural material in fluid has been reported. According to the benchmark of the oxygen diffusion process with the analytical solution and the reported numerical solutions from other research group, it shows that the developed CA model significantly consists in the anticipated estimation of the transport of oxygen at a mesoscopic level. To promise the homogeneous and isotropic macroscopic properties, a uniform developing probability in each direction and a synchronous dynamics scheme with random selection in the whole simulation domain has been adopted. The basic ideas of the developed model have been designed to satisfy the mass transport, corrosion, and oxidation mechanisms of stainless steels in LBE environment. The averaging mesoscopic probabilities have been mapped with the macroscopic properties by some fitting schemes and the results are benchmarked with the experimental data. This paper presents an initial study of the corrosion/oxidation process of nickel based metal, Inconel 625 superalloy, in supercritical water by CA model. The main purpose of this paper is to provide the initial study of the corrosion and oxidation process from a mesoscopic level on one hand, and we hope to setup a tool which can provide the guidance for design, optimization and testing of the coolant system in advanced nuclear reactor in the future on the other hand.

2. Prevoius CA model

2.1. An improved mesoscopic oxidation (IMO) CA model

The main difference between an improved mesoscopic oxidation (IMO) CA model and the traditional CA models proposed by Saunier (Saunier et al., 2004) is that the interstitial sites and the grain boundary have been proposed to be the pathway of oxygen transport (Tan et al., 2008c). The state of a given site in the next time step will be determined by the state of itself and its neighbors at the previous time step. The control variables can be formulated as follows:

$$Inte_{i,j}(t+\delta t) = \Phi_{Inte}\left(Inte_{i,j}(t), \left\{Inte_{i,j}^{Nb}(t)\right\}, \left\{Lat_{i,j}^{Nb}(t)\right\}, \varphi_{Inte}\right) \quad (1)$$

$$Lat_{i,j}(t+\delta t) = \Phi_{Lat}\left(Lat_{i,j}(t), \left\{Lat_{i,j}^{Nb}(t)\right\}, \left\{Inte_{i,j}^{Nb}(t)\right\}, \varphi_{Lat}\right) \quad (2)$$

where Φ_{Lat} and Φ_{Inte} are the local evolution rules of CA for lattice sites and interstitial sites, respectively. φ_{Lat} and φ_{Inte} are the control variables for lattice sites and interstitial sites, respectively. There are eight neighbor lattice sites$\{Lat_{i,j}^{Nb}(t)\}$ and four neighbor interstitial sites $\{Inte_{i,j}^{Nb}(t)\}$ for each lattice site, $Lat_{i,j}^{Nb}(t)$. Similarly, there are four neighbor lattice sites and four neighbor interstitial sites for each interstitial site $Inte_{i,j}(t)$ in the 2D CA model. The basic rules of the transport and diffusion of each species in simulation domain for the IMO CA model can be found in our previous publication (Tan et al., 2008c). Ions of metals diffuse N_{WD} steps after N_{OT} steps of transport of oxygen in the oxide layer. The ratio of transport steps, K_d (=N_{OT}/N_{WD}), an important explicit parameter, which depends on the mass transport rate of oxygen and ionic metal in the oxide layer, has been introduced. Another important implicit parameter, P_{act}, is assigned as the probability of each reaction.

2.2. An improved mesoscopic oxidation (IMO) CA model coupling with a simple scale removal (SSR) model

Considering the scale removal effect of the oxidation layer, a constant removing probability is assigned for each oxide lattice as the oxide lattice is contacting with the LBE lattice. The removing probability is assumed to be zero in the SSR model, if the oxide cell does not contact with any LBE lattice. Consequently, the scale removal condition will be examined and processed only if there is a cell occupied by fluid above cell occupied by oxide which satisfies the scale removal condition after every step of chemical reaction procedure.

2.3. An improved mesoscopic oxidation (IMO) CA model coupling with a improved scale rem1 oval (ISR) model

The CA model is improved to consider the effect from the flow direction based on the previous model. The proposed improved scale removal (ISR) model can setup a basis for the future study of corrosion and erosion on the stainless steel. The scale removing probability influenced by the surrounding neighboring lattices (the eastern, western, northern, northeastern, and northwestern lattices) of the objective oxide layer site is taken into consideration, which is based on the estimation of the hydraulic effect. The scale removal probability averaged from the total possible cases equal to $\overline{P_{Kr}}$. The scale removal probability for each cell can be expressed as, $P_{Kr}^{i} = f_i\overline{P_{kr}}$, where f_i is a factor describing that how difficult the objective oxide cell will be removed. A low value of f_i stands for high difficulty by which the cell will be removed. Apparently, $1/Q\sum_{i}^{Q} f_i = 1$, where, Q is the total number of the possible cases. In a 2D domain, the details of possible cases for sites on the oxide surface and the assigned factors f_i are listed in our previous study (Tan and Chen, 2009b).

3. The IMO CA model with ISR model considering the effect of spinel by adding chromium

In this improved CA model, the formation of spinel will be studied as a result of adding alloying element chrome in the structural material. This model is developed based on the IMO CA model with ISR model mentioned above. Hence, the scale removal effect is still involved in this model. The added alloying element, chromium, has a different reaction probability with oxygen compared with the main content of nickel in Inconel 625. The scale removal coefficient is related to effect of hydraulic effect on different roughness of the oxide surface in ISR model. Comparing experimental results in SCW (Huang et al., 2009) and in LBE (Zhang et al., 2005), the thickness of oxide layer of Inconel 625 was in the same order as that of stainless steel observed after the same testing time. Therefore, low reaction probability and low average scale removal probability in previous CA model for LBE was adapted in this CA model for SCW. With this new model, the effect of the added alloying element, chromium, on the oxidation process can be studied. Besides the chromium, the main element of structure material and working fluid in this model are modified by nickel and supercritical water respectively to match the reaction system which is the Inconel 625 superalloy in the SCW. The schematic plot of the developed CA model is modified as shown in Fig. 1. The state of each square cell was represented by the site variable Lat_x, which denotes a different component at a site. Lat_2

represents the atomic nickel site. Lat_3 denotes the supercritical water site (liquid phase). Lat_4 denotes site of the nickel oxide. Lat_5 means "walker," the site of ionic nickel overlapping with oxide. Lat_6 denotes the atomic chrome site. Lat_7 denotes the spinel site. With the appearance of the added chromium, the spinel sites will be formed, which consists of the chromatic oxide and nickel oxide.

The basic rules for this CA model are mentioned in section 2.1 and our previous study (Tan et al., 2008c). The local developing rules for the CA model will be modified according to results of our laboratory experiments (Huang et al., 2009). The formation of spinel will occur with a reaction probability only if chrome, nickel and oxygen exist at the neighboring lattice. To simulate the growth of spinel along the same direction as the oxide layer growth direction, two different reaction probabilities are assigned. One probability, $P_{actspTB}$ is for the spinel growth in *y*-direction, along the oxide layer growth direction; another one, $P_{actspLR}$ is for the spinel growth in *x*-direction, perpendicular to the *y*-direction. The average value of this two probability in *x*- and *y*-direction equals to the total spinel chemical reaction probability P_{actsp}. With the improved CA oxidation model, the oxidation process can be studied at the mesoscopic level considering the formation of the spinel consisted from nickel, chrome and oxygen. In the present study, the influence of chromium and scale removal effect by the hydraulic effect resulting from the roughness of the interface of fluid and oxide layer has been taken into consideration at the same time.

4. Results and discussion

The oxidation process of the alloy consisted in nickel and the alloying element, chrome, has been investigated in a 2-D domain of 500 (a [m]) ξ500 (a [m]). Based on the experimental environment of supercritical water at 600 °C and 24.8 MPa, and the inlet oxygen concentration in supercritical was controlled at the level of 8.3 ppm. The thickness of oxide layer of Inconel 625 superalloy was 27, 81, 660, 880 and 1280 nm at 600 °C and 24.8 MPa supercritical water for 24, 100, 300, 600, and 1000 h, respectively (Huang et al., 2009). Because of the oxygen concentration was controlled in experiment, the oxygen was assumed to be stable and will be supplied immediately after reaction in supercritical water (SCW) region and thus the C_{ox} was set to be 0.2 (Tan et al., 2008c; Tan and Chen, 2009b). The C_{ox} is the parameter of oxygen concentration in this CA model. C_{ox} is set to be 0.2 because the CA model focused on the coolant system where oxygen concentration in working flow was controlled at a constant level and enough oxygen for oxidation can be acquired. The chemical reactive probability between nickel and oxygen, P_{act}, is set to be 0.005. The value of the reaction probability, P_{act}:0.005, denotes the oxidation with low reaction probability where the transport of oxygen exceeds the consumption of oxygen during the oxidation reaction. The content of chrome, C_{cr}, is 0.23 to match the composition of the Inconel 625 superalloy. Considering the assumption in which the transportation rate of oxygen into oxide layer is faster than the outward diffusion rate of the metal ion to the SCW, the transport ratio K_d is set to be 2. K_d:2 indicates that the step of transport of oxygen was twice the step of diffusion of walker." The volume control parameter ε is set to be unity. The time interval, Δt, is set to be 0.05 h (=180 s), and the width of a square cell in CA model, a, is set to be 19 nm. The water flow is assumed to flow from left to right.

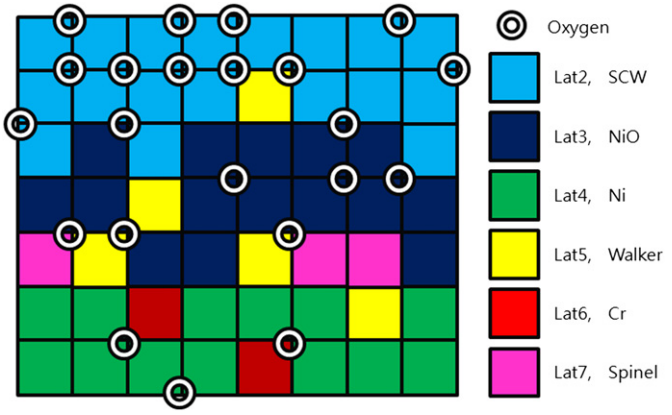

Fig. 1. Schematic plot of the CA model with added element chrome.

The formation of spinel and the hydraulic effect do significant influence on the growth of oxide layer, four cases with specific reaction probability and specific scale removal probability was chose in this study. The spinel reaction probability in *x*-direction, *y*-direction, and average scale removal probability in Case 1 is PactspLR = 5×10^{-6}, PactspTB = 1.5×10^{-5} and $\overline{P}_{Kr} = 0.0001$; in case 2 is PactspLR = 5×10^{-5}, PactspTB = 1.5×10^{-4} and $\overline{P}_{Kr} = 0.0001$; in case 3 is PactspLR = 5×10^{-6}, PactspTB = 1.5×10^{-5} and $\overline{P}_{Kr} = 0$,respectively. The reaction probabilities in case 4 were all the same as those in case 1, except for the K_d, which is set to at 0.5. Fig. 2 depicted the thickness of the oxide layer simulated by our CA model in the four cases and the value measured from laboratory experiment (Huang et al., 2009). Comparing to thickness of the oxide layer in case 1 with lower chemical reaction probability of the spinel and case 2 with higher ones, people can easily found the fact thickness in case 1 was larger than that in case 2. The root cause to the difference of the thickness would be related with the microstructure and may be explained by the snapshot of the simulation in case 1 (left) and case 2 (left) at $N_t = 5000$, as shown in the half of the left side and right side of Fig. 3(a). The zone in view of case 1 in Fig. 3(b) and case 2 in Fig. 3(c) demonstrates a denser spniel structure and a thinner oxide layer as the reaction probability of spinel is high. The density of spinel in this 2D model can be represented by the percentage of spinel sites as depicted in Fig. 4 which present a denser spinel in case 2 than in case 1. The denser spinel structure makes the outward diffusion of nickel ion difficult and then reduces the chance of the reaction between nickel ion and oxygen. Thus, the lower oxide layer in the case with higher chemical reaction probability is observed.

Comparing the scale removal effect on the thickness of oxide layer, results of case 1 considering the scale removal effect

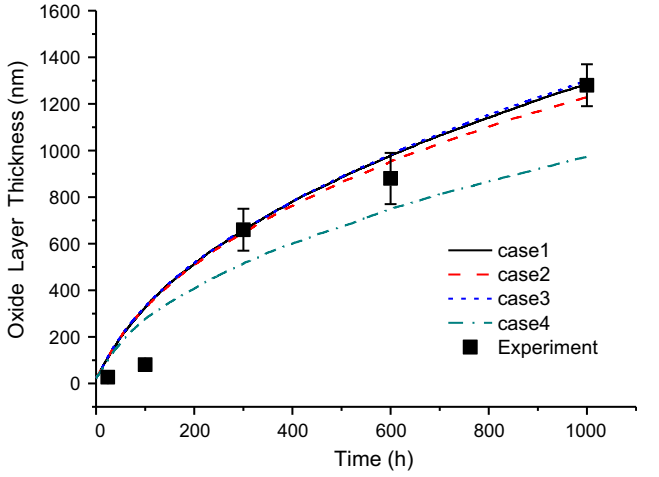

Fig. 2. The comparison of thickness of the oxide layer simulated by CA model in case 1 ($P_{actspLR} = 5 \times 10^{-6}$, $P_{actspTB} = 1.5 \times 10^{-5}$, $\overline{P}_{Kr} = 0.0001$ and $K_d = 2$), case 2 ($P_{actspLR} = 5 \times 10^{-6}$, $P_{actspTB} = 1.5 \times 10^{-5}$, $\overline{P}_{Kr} = 0.0001$ and $K_d = 2$), case 3 ($P_{actspLR} = 5 \times 10^{-6}$, $P_{actspTB} = 1.5 \times 10^{-5}$, $\overline{P}_{Kr} = 0$ and $K_d = 2$) and case 4 ($P_{actspLR} = 5 \times 10^{-6}$, $P_{actspTB} = 1.5 \times 10^{-5}$, $\overline{P}_{Kr} = 0.0001$ and $K_d = 0.5$) and the value measure from laboratory experiment.

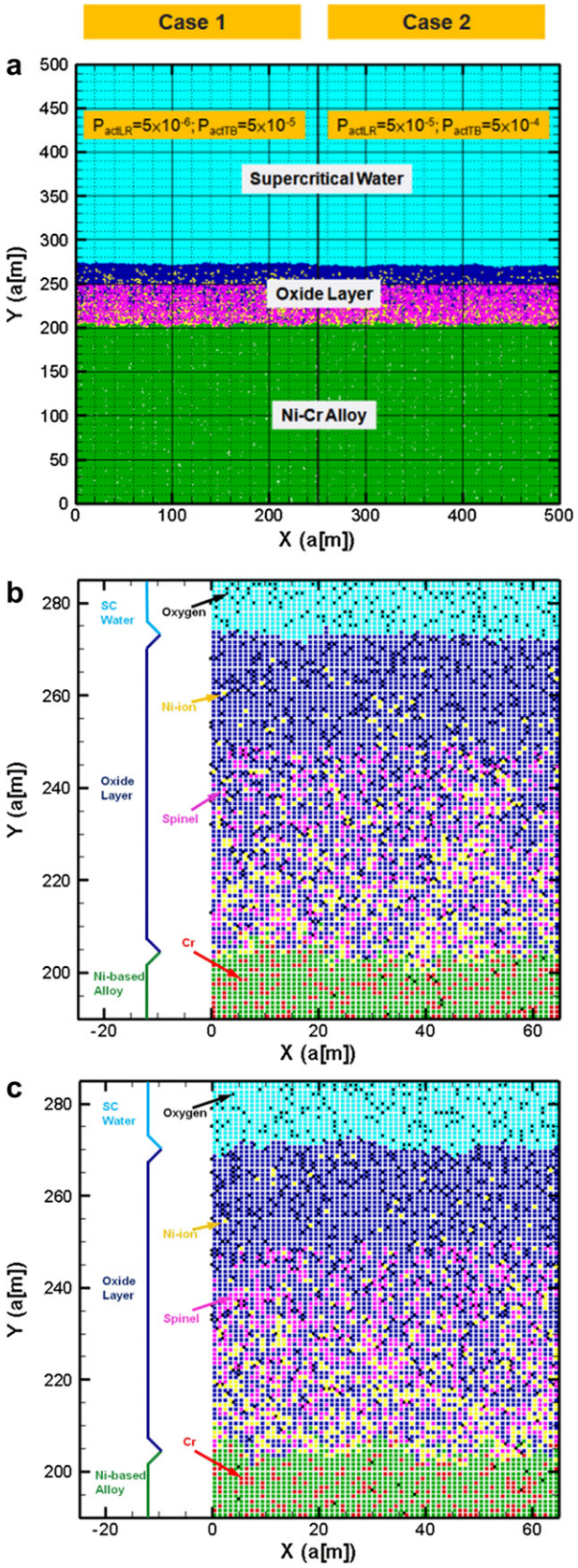

Fig. 3. (a) Snapshot of the oxidation process, C_{cr} = 23%, C_{ox} = 0.2, P_{act} = 0.005, and $\overline{P}_{Kr}$ = 0.0001, for time steps N_t = 5000. Left case (case 1): $P_{actspLR} = 5 \times 10^{-6}$ and $P_{actspTB} = 1.5 \times 10^{-5}$. Right case (case 2): $P_{actspLR} = 5 \times 10^{-5}$ and $P_{actspTB} = 1.5 \times 10^{-4}$., (b) Zone in view of snapshot of the left case (case 1) in (a), and (c) Zone in view of snapshot of the right case (case 2) in (a).

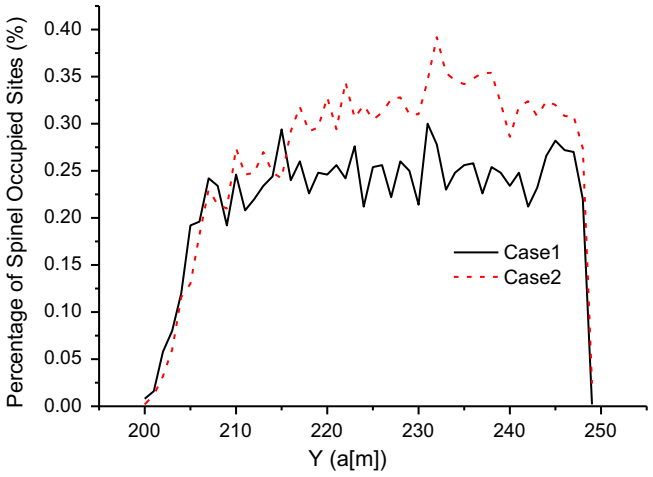

Fig. 4. The spinel concentration in the oxide layer.

($\overline{P}_{Kr}$ = 0.0001) and results of case 3 neglecting the scale removal effect ($\overline{P}_{Kr}$ = 0) were shown in Fig. 5. The growth rate of oxide layer in both case are very close and they both almost match the experimental data. The difference of oxide layer growth rate between two cases can only be observed for quite a long time of oxidation. This result implies that the scale removal effect of the Inconel 625 in such supercritical water is hard to be observed under limited experimental period, and it could cause unpredictable problem for long service time. A well developed CA model considering with scale removal effect would be helpful to study this kind of issue. The oxide layer's thickness in case 1 (K_d = 2) and case 4 (K_d = 0.5) shows significant deviation. The oxide layer in case 4 was much thinner than that in case 1. This CA model proposes that the oxygen in supercritical water will transport into oxide and the metal along the grain boundary of the oxide and structural material or vacancies of the oxide and metallic lattice. Moreover, the outward diffusion of the ionic metal species which also results in the formation the oxide in the interface of oxide layer and metal region was included in the CA model. The results presented that the mobility of oxygen is higher than ionic metal when the oxidation occurring. By means of the CA model, the thickness of the duplicate oxide layer agrees with the observation of the laboratory experiment (Huang et al., 2009). The trend of growth of the oxide layer follows the parabolic law.

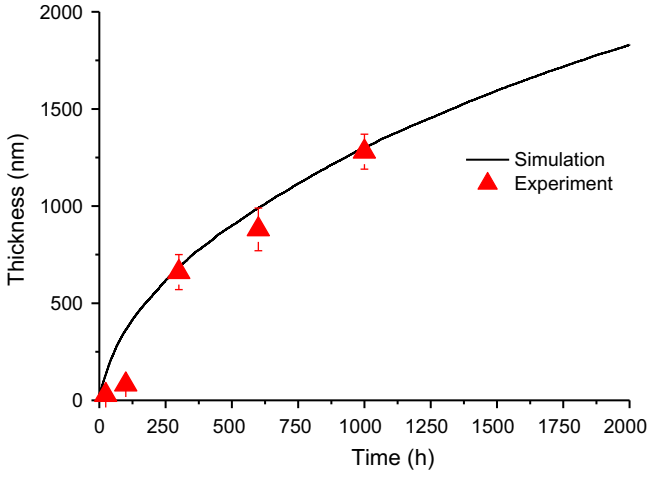

Fig. 5. Comparison of the fitted results and the experimental data (Huang et al., 2009).

Finally, growth of oxide layer in case 1 agreed the experimental results the most after analyzing the simulating results in four cases. In Fig. 5, the oxide thickness from experimental data and the prolonged simulation of the oxide layer growth of Inconel 625 superalloy in 600 °C and 24.8 MPa supercritical water are demonstrated. With good agreement between simulation results and laboratory experimental results has been obtained from 0 to 1000 h, as shown in Fig. 5, one can predict the oxide layer thickness for 2000 h can be estimated to be 1831 nm by means of the present CA model.

5. Conclusions

The cellular automaton oxidation model in 600 °C 24.8 MPa SCW has been proposed considering formation of NiO and spinel of nickel oxide and chrome oxide, by the added alloying element, chrome. The scale removal effect has been taken into account in the present model. With the developed CA oxidation model, the oxidation process has been investigated, in which the formation of spinel of chrome oxide and nickel oxide has been involved, at a mesoscopic level. A scheme to control the growth of the spinel has been proposed in the CA model. The duplicate oxide layer in the CA model fits the experimental observation of the oxide structure of Inconel 625 superalloy. The trend of the simulated results from the CA model and experimental results follows the parabolic law. With this scale removal CA model, it help us to predict and estimate the oxide layer of the Inconel 625 in SCW at such high temperature, 600 °C, and such high pressure, 24.8 MP.

Nomenclature

a	width of a square lattice in CA model in unit of meters
C_{ox}	statistic oxygen concentration in supercritical water
C_{cr}	statistic chrome concentration in nickel alloy
f_i	scale removal difficulty factor
$Inte_{i,j}(t)$	state variable of the interstitial sites
$Inte_{i,j}^{Nb}(t)$	state variable of the neighbor interstitial sites of the lattice (i, j)
$Lat_{i,j}(t)$	state variable of the lattice site
$Lat_{i,j}^{Nb}(t)$	state variable of the neighbor lattice sites of the lattice (i, j)
P_{kr}	scale removing probability for SSR (simple scale removal) model
$\overline{P}_{Kr}$	average scale removal probablity
P_{act}	reaction of probability of oxygen sites and metal sites
PactspTB	the spinel chemical reaction probability in *y*-direction
PactspLR	the spinel chemical reaction probability in *x*-direction
Q	the total number of the possible cases in the ISR model
Δt	time interval of formation of the oxide layer between two steps
ε	volume control parameter
Φ_{Lat}	local evolution rules for a lattice site
Φ_{Inte}	local evolution rules for an interstitial site
φ_{Lat}	control variables for an interstitial site
φ_{Inte}	control variables for a lattice site

References

Eden, M., 1961. Proc. 4th Berkeley Symposium on Mathematics, Statistics and Probability. In: Neyman, F. (Ed.), A Two-dimensional Growth Process, In: Biology and Problems of Health, vol. 4. University of California Press, Berkeley, pp. 223–239.

Huang, Z.C., Kai, J.J., Chen, F.Z., Yeh, T.K., 2009. Corrosion behavior of Inconel 625 superalloy in supercritical water. Master Thesis. National Tsing Hua Univeristy.

Otsuka, N., Fujikawa, H., 1991. Scaling of austenitic stainless steels and nickel-base alloys in high-temperature steam at 973 K. Corrosion 47, 240–248.

Saunier, J., Chausse, A., Stanfiej, J., Badiali, J.P., 2004. Simulations of diffusion limited corrosion at the metal/environment interface. J. Electroanal. Chem. 563, 239–247.

Sun, M., Wu, X., Zhang, Z., Han, E.H., 2008. Analyses of oxide films grown on alloy 625 in oxidizing supercritical water. J. Supercrit. Fluids 47, 309–317.

Tan, T., Chen, Y.T., 2009a. Simulations of metal oxidation in LBE at a mesoscopic level. J. Eng. Gas. Turbines Power-Trans. ASME 131, 032903–032909.

Tan, T., Chen, Y.T., 2009b. Scale removal cellular automaton oxidation models of metals in lead bismuth eutectic. J. Electroanal. Chem. 626, 89–97.

Tan, L., Ren, X., Sridharan, K., Allen, T.R., 2008a. Corrosion behavior of Ni-base alloys for advanced high temperature water-cooled nuclear plants. Corros. Sci. 50, 3056–3062.

Tan, T., Chen, Y.T., Chen, H., 2008b. A diffusion controlling duplex-layer oxidation model with scale removal in oxygen containing liquid metal flow. Comput. Mater. Sci. 44, 750–759.

Tan, T., Chen, Y.T., Chen, H., 2008c. An improved mesoscopic oxidation model of metals in molten lead or LBE. Comput. Mater. Sci. 43, 251–267.

Wasa, G.S., Ampornrat, P., Gupta, G., Teysseyre, S., West, E.A., Allen, T.R., Sridharan, K., Tan, L., Chen, Y., Ren, X., Pister, C., 2007. Corrosion and stress corrosion cracking in supercritical water. J. Nucl. Mater. 371, 176–201.

Zhang, J.S., Li, N., Chen, Yitung, Rusanov, A.E., 2005. J. Nucl. Mater. 336, 1–10.